Fabrication of $BaTi_2O_5$ Glass−Ceramics with Unusual Dielectric Properties during Crystallization

Jianding Yu,*,† Yasutomo Arai,† Tadahiko Masaki,† Takehiko Ishikawa,† Shinichi Yoda,† Shinji Kohara,‡,§ Hiroshi Taniguchi,|| Mitsuru Itoh,|| and Yoshihiro Kuroiwa§,⊥

Japan Aerospace Exploration Agency, ISS Science Project Office, 2-1-1 Sengen, Tsukuba, Ibaraki 305-8505, Japan, Japan Synchrotron Radiation Research Institute, 1-1-1 Kouto, Sayo-cho, Sayo-gun, Hyogo 679-5198, Japan, CREST, Japan Science and Technology Agency, Honmachi, Kawaguchi, Saitama 332-0012, Japan, Materials and Structures Laboratory, Tokyo Institute of Technology, 4259 Nagatsuta, Midori-ku, Yokohama 226, Japan, and Graduate School of Science, Hiroshima University, 1-3-1 Kagamiyama, Higashi-hiroshima, 739-8526, Japan

Received November 19, 2005. Revised Manuscript Received February 20, 2006

A 2-mm-diameter glass sphere of ferroelectric $BaTi_2O_5$ was fabricated from melt using containerless processing. The glass structure was analyzed by high-energy X-ray diffraction using an incident photon energy of 113.5 keV, indicating that distorted Ti−O polyhedra, with average coordination number (N_{Ti-O}) of approximately 5, presented in the glass. Above the glass transition temperature (972 K), three successive phase transitions, from glass to a metastable α phase at 972 K, then to a metastable β phase at 1038 K, and finally to a stable monoclinic γ phase above 1100 K, were observed. At the crystallization temperature of the α phase, the permittivity jumped instantaneously by more than 1 order of magnitude, reaching a peak of 1.4×10^7. This interesting phenomenon, occurring near the crystallization temperature, has important technical implications for obtaining an excellent dielectric glass−ceramic through controlled crystallization of $BaTi_2O_5$ glass.

Introduction

Recently, much effort has been devoted to forming bulk glass from the melt of ferroelectric crystalline materials ($BaTiO_3$, $PbTiO_3$, $LiNbO_3$) without adding any network-forming oxides such as SiO_2 because of the potential for producing transparent glass−ceramics with high dielectric constants and enhanced piezoelectric, pyroelectric, and electro-optic effects.[1−3] However, this requires a cooling rate higher than that of glass formed by conventional techniques. Therefore, only amorphous thin films have been formed, using rapid quenching with a cooling rate $> 10^5$ K/s.[4−7] Thin films are generally very brittle and heterogeneous in microstructure and, thus, are of limited practical use. The amorphous thin film of the ferroelectric material $LiNbO_3$ prepared by Glass et al.[4] exhibited a pronounced dielectric anomaly with a permittivity peak of $\epsilon' > 10^5$ close to the crystallization temperature. Lines' theory explained this anomaly as a ferroelectric-like transition in the amorphous state, based on the assumption that the reorientation of the distorted soft units could cause considerable polarization.[8] However, the Maxwell−Wagner effect caused by structural inhomogeneities, which appeared just before crystallization due to the formation of small clusters of a new crystal phase, would also contribute considerably to the anomalous permittivity.

Because the containerless processing prevented melt contamination, minimized heterogeneous nucleation, and allowed the melt to achieve deep undercooling for glass forming, we were able to successfully fabricate a bulk ferroelectric barium titanate oxide glass, $BaTi_2O_5$, with a ferroelectric phase transition of $T_c = 703$ K[9,10] from melt. A 2-mm-diameter glass sphere was formed using containerless processing. To our knowledge, this was the first time that a bulk glass of ferroelectric material was fabricated from melt without adding any network-forming oxide. We anticipate the bulk ferroelectric glass to be not only an excellent candidate for practical material but also an ideal model material for fundamental research in ferroelectric and optical physics. Our report includes some interesting dielectric properties of the $BaTi_2O_5$ glass at crystallization temperature, such as the instantaneous jump of permittivity to greater than the 10^7 observed at the crystallization temperature. The origin of the giant permittivity in the glass was discussed in terms

* Corresponding author. E-mail address: yo.kentei@jaxa.jp.
† Japan Aerospace Exploration Agency.
‡ Japan Synchrotron Radiation Research Institute.
§ Japan Science and Technology Agency.
|| Tokyo Institute of Technology.
⊥ Hiroshima University.

(1) Narasaki, A.; Tanaka, K.; Hirao, K. *Appl. Phys. Lett.* **1999**, *75*, 3399.
(2) Sakai, R.; Benino, Y.; Komatsu, T. *Appl. Phys. Lett.* **2000**, *77*, 2118.
(3) Takahashi, Y.; Benino, Y.; Fujiwara, T.; Komatsu, T. *Appl. Phys. Lett.* **2002**, *81*, 223.
(4) Glass, A. M.; Lines, M. E.; Nassau, K.; Shiever, J. W. *Appl. Phys. Lett.* **1977**, *31*, 249.
(5) Nassau, K.; Wang, C. A.; Grasso, M. *J. Am. Ceram. Soc.* **1979**, *62*, 74.
(6) Masaaki, T.; Nakamura, T.; Tsuya, N.; Arai, K.; Ozawa, H.; Uno, R. *Jpn. J. Appl. Phys.* **1980**, *19*, 555.
(7) Kim, S. H.; Chae, B. G.; Yang, Y. S.; Lee, S. J.; Kim, J. P. *Jpn. J. Appl. Phys.* **1998**, *37*, 234.
(8) Lines, M. E. *Phys. Rev. B.* **1978**, *17*, 1984.
(9) Akishige, Y.; Fukano, K.; Shigematsu, H. *Jpn. J. Appl. Phys.* **2003**, *42*, L946.
(10) Waghmare, U.; Sluiter, M. H. F.; Kimura, T.; Goto, T.; Kawazoe, Y. *Appl. Phys. Lett.* **2004**, *84*, 4917.

10.1021/cm0525555 CCC: $33.50
Published on Web 03/17/2006

of Lines' model and the Maxwell−Wagner effect. A good fit of the anomalous dielectric data at crystallization with Lines' model was obtained, suggesting that reorientation of the distorted Ti−O polyhedra in a glassy matrix between a random and an ordered state may yield ferroelectric-like behavior at the crystallization temperature. However, impedance measurement data reveal that two phases with significantly different conductivities coexist at crystallization, indicating that the giant permittivity during crystallization could also be explained by structural inhomogeneity.

An academic interest of the present study resides in the fact that a single monoclinic $BaTi_2O_5$ phase could not be prepared by conventional solid-state reaction but could only be synthesized from a melt or amorphous state,[11−15] and its thermal stability still remains uncertain. Rase and Roy indicated that $BaTi_2O_5$ could be stable over a temperature range from the solidus of 1595 K to 1483 K.[11] However, other reports have indicated that $BaTi_2O_5$ would decompose to $BaTiO_3$ and $Ba_6Ti_{17}O_{40}$ in such a temperature range.[12−15] The results of our differential scanning calorimetry (DSC) and X-ray diffraction analysis revealed that two new intermediate phases (defined as the α and β phases) presented above the crystallization temperature. The monoclinic $BaTi_2O_5$ (defined as the γ phase) was translated from the α and β phases and could remain stable up to 1553 K.

It was found that the permittivity reached its maximum value only when the α phase crystallized from a glass matrix and that the permittivity decreased when α phase disappeared. This gave rise to an important technical implication for obtaining excellent dielectric glass−ceramics through controlled crystallization of $BaTi_2O_5$ glass.

Experimental Section

Synthesis. Containerless processing is an attractive synthesis technique, as it provides a possibility to solidify the undercooled liquid into a selected phase to synthesize materials with desired structures and novel properties.[16,17] $BaTi_2O_5$ glass spheres (2-mm diameter) were fabricated using containerless processing in an aerodynamic levitation furnace (ALF).[18,19] High-purity commercial $BaTiO_3$ and TiO_2 powders were mixed with a mole ratio of 1:1, compressed into rods under a hydrostatic pressure of 200 MPa, and then sintered at 1427 K for 10 h. Bulk samples with a mass of about 10 mg were cut from the rods, levitated with the ALF, and then melted by a continuous-wave CO_2 laser beam. A pyrometer was utilized to measure the temperature of the sample. A high-resolution charge-coupled device video camera equipped with a telephoto objective lens was employed to obtain a magnified view of the sample. Laser power was used to carefully bring the sample to the desired temperature prior to quenching. After quenching at a cooling rate of about 1000 K/s, 2 mm diameter glass spheres could be obtained.

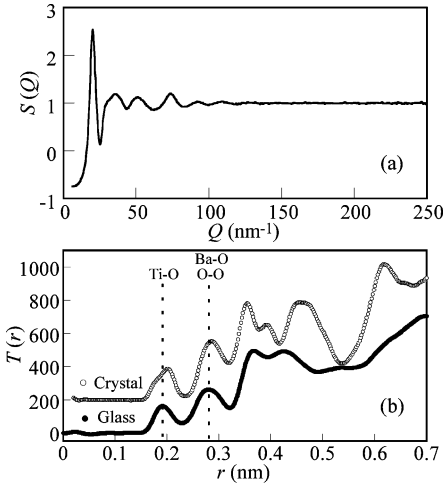

Figure 1. (a) Total structure factor $S(Q)$ of $BaTi_2O_5$ glass. (b) Total correlation functions $T(r)$ of $BaTi_2O_5$ crystal and glass. Dashed lines are a guide to the eye.

Characterization. To analyze the glass structure, a high-energy X-ray diffraction experiment was performed using an incident photon energy of 113.5 keV at the high-energy X-ray diffraction beamline BL04B2[20] of SPring-8, with a two-axis diffractometer for the disordered materials.[21] Two glass spheres mounted on a silica glass capillary were measured for 12 h. The X-ray diffraction pattern of a 2-mm-diameter glass sphere was measured in transmission geometry up to $Q = 250$ nm^{-1}. The analysis was performed as described elsewhere.[21]

The glass-transition behavior was studied by DSC with a heating rate of 10 K/min from room temperature to 1600 K. The structure changes during heating were characterized by powder X-ray diffraction using Cu Kα radiation with two sequences. One was to measure the glassy powder at various heating temperatures in the temperature range from room temperature to 1100 K, and the other was to measure the powder after it was annealed at various temperatures in the temperature range from 900 to 1600 K. To refine the structure of the crystals crystallized from glass, some powder samples were also measured using high-energy X-ray diffraction of 25 keV in beamline BL02B2 of SPring-8. For electrical property measurements, we cut and ground the samples into disks of 0.3−0.4 mm thickness and measured the dielectric constant and impedance from room temperature to 1123 K at a heating rate of 3 K/s using Ag electrodes.

Results and Discussion

Glass Structure. A preliminary study of the glass structure of $BaTi_2O_5$ was performed by high-energy X-ray diffraction. Figure 1a illustrates the X-ray structure factor $S(Q)$ as functions of the wave vector of the bulk $BaTi_2O_5$ glass. The Q position of the first sharp diffraction peak is at 20 nm^{-1}, which is similar to the position of that in K_2O-TiO_2 glass.[22] Figure 1b depicts the derived total correlation function $T(r)$ of the bulk $BaTi_2O_5$ glass, comparing it to that of monoclinic

(11) Rase, D. E.; Roy, R. *J. Am. Ceram. Soc.* **1955**, *38*, 102.
(12) Jonker, G. H.; Kwestroo, W. *J. Am. Ceram. Soc.* **1958**, *41*, 390.
(13) Negas, T.; Roth, R. S.; Parker, H. S.; Minor, D. *J. Solid State Chem.* **1974**, *9*, 249.
(14) O'Bryan, H. M.; Thomson, J. *J. Am. Ceram. Soc.* **1974**, *57*, 522.
(15) Ritter, J. J.; Roth, R. S.; Blendell, J. E. *J. Am. Ceram. Soc.* **1986**, *69*, 155.
(16) Yu, J.; Paradis, P.-F.; Ishikawa, T.; Yoda, S.; Saita, Y.; Itoh, M.; Kano, F. *Chem. Mater.* **2004**, *16*, 3973.
(17) Yu, J.; Paradis, P.-F.; Ishikawa, T.; Yoda, S. *Appl. Phys. Lett.* **2004**, *85*, 2899.
(18) Yu, J.; Paradis, P.-F.; Ishikawa, T.; Yoda, S. *Jpn. J. Appl. Phys.* **2004**, *43*, 8135.
(19) Paradis, P.-F.; Babin, F.; Gagne, J.-M. *Rev. Sci. Instrum.* **1996**, *67*, 262.
(20) Isshiki, M.; Ohishi, Y.; Goto, S.; Takeshita, K.; Ishikawa, T. *Nucl. Instrum. Methods Phys. Res., Sect. A* **2001**, *467*, 663.
(21) Kohara, S.; Suzuya, K.; Kashihara, Y.; Matsumoto, N.; Umesaki, N.; Sakai, I. *Nucl. Instrum. Methods Phys. Res., Sect. A* **2001**, *467*, 1030.
(22) Sakka, S.; Miyaji, F.; Fukui, K. *J. Non-Cryst. Solids* **1989**, *107*, 171.

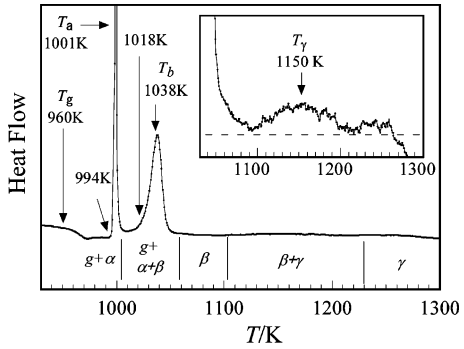

Figure 2. DSC heating profiles of $BaTi_2O_5$ glass, showing the glass phase transition and three successive phase transitions.

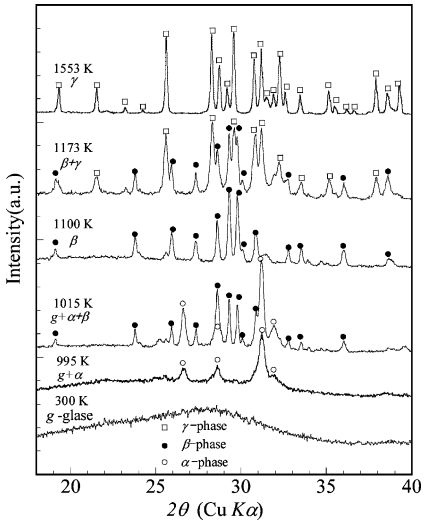

Figure 3. X-ray diffraction patterns of $BaTi_2O_5$ glass at various temperatures, showing the glass phase and three crystal phases.

$BaTi_2O_5$ crystal with space group of $C121$.[23] The $T(r)$ of the crystal was calculated using the PDFFIT computer code.[24] The Ti−O peak of the glass was observed at 0.192 nm in $T(r)$, whereas the crystalline $BaTi_2O_5$ exhibits two Ti−O distances at $r < 0.20$ nm and four distances at $r > 0.20$ nm. This short-range difference of Ti−O distances between crystalline and glassy $BaTi_2O_5$ was also observed in forsterite (Mg_2SiO_4) crystal and glass, which can be synthesized using containerless processing.[25] The Ti−O peak of the glass at 0.192 nm is broad and skewed toward the low-r side, suggesting the existence of highly distorted polyhedra formed by the distribution of Ti−O bond lengths. The average coordination number N_{Ti-O} obtained from a fitting Ti−O peak using Gaussian functions is approximately 5. This indicates that the network former in the glassy state is mainly contributed to by distorted [TiO_5] polyhedra. According to Lines' model,[8] the distorted Ti−O polyhedra can be considered as dielectrically soft units, which randomly oriented in a glassy matrix. Considerable polarization in long-range order would be caused by reorientation of the distorted soft units at crystallization temperature. As it will be mentioned below, an instantaneous jump of permittivity to greater than the 10^7 occurred at the crystallization temperature and it was well-fitted with Lines' model. The magnitude of the peak at around 0.28 nm, which was mainly due to Ba−O and O−O correlations in $T(r)$ of crystal, decreased in glass, implying that the distribution of Ba ions in the glass state is more disordered than in the crystalline state.

Crystallizations. Figure 2 illustrates the thermal stability of the glass studied by DSC. From an endothermic anomaly in the DSC heating curve, we determined the onset and end temperatures of glass transition as 960 K ($T_{g-onset}$) and 972 K (T_{g-end}). After the glass transition, we observed three exothermic peaks: a large, sharp peak at $T_\alpha = 1001$ K; a smaller peak at $T_\beta = 1038$ K; and a broad, weak peak around $T_\gamma = 1150$ K (inset, Figure 2). After the glass transition, T_α was attributed to crystallization from the glassy matrix, and the onset temperature of crystallization, $T_{\alpha-onset}$, was estimated as 994 K. Following the glass transition and crystallization, T_β and T_γ could be attributed to either new crystallization from the glassy matrix or a polymorphic transition of the newly formed crystal. To resolve this, we performed X-ray diffractions for the samples after heating them to high temperatures (Figure 3). The as-cooled sample displayed a typical amorphous diffraction pattern. When samples were heated to 995 K ($T_{\alpha-onset}$), several diffraction peaks appeared on the baseline of a hollow curve, indicating that a crystal, defined as α phase, had formed from the glass matrix. When the temperature was raised to 1015 K (above the T_α peak), numerous new diffraction peaks appeared in addition to the peaks of the α phase. The additional diffraction peaks revealed a new phase, defined as the β phase. When the sample was heated to 1100 K (above the T_β peak), the X-ray diffraction pattern displayed a single β phase. This indicated that the α phase gradually translated to the β phase in the temperature range of T_α to T_β. When the temperature reached 1173 K (around T_γ), the β phase began to translate to another new phase, defined as the γ phase, and became a single γ phase at 1553 K. The crystal structure of the γ phase was refined by Rietveld profile fitting using the data measured with synchrotron radiation to identify the structure of the γ phase as a monoclinic structure with a space group of $C121$ and lattice parameters as $a = 1.68992(2)$ nm, $b = 0.39368(1)$ nm, $c = 0.94141(1)$ nm, and $\beta = 103.1004(8)°$, which was consistent with the result of the single crystal.[23] However, we could not identify the structures of the α phase and β phase based on the reported BaO−TiO_2 compounds, suggesting that both phases were new metastable crystals. Hence, we attributed the exothermic peaks of T_β and T_γ to two polymorphic transitions of $BaTi_2O_5$ and estimated the onset temperature as $T_{\beta-onset} = 1018$ K and $T_{\gamma-onset} = 1100$ K.

Permittivity. Figure 4 depicts the temperature dependence of the permittivity ϵ' and the loss component tan δ for the glass sample during heating from room temperature to 1100 K. At room temperature, magnitudes of ϵ' over a frequency range of 100 to 1 M Hz were less than 100, and those of tan δ were less than 0.01. The temperature dependencies of ϵ' and tan δ weakened below 800 K and strengthened above 800 K. The magnitude of ϵ' at a frequency of 100 Hz increased from 10^2 to 10^6 with increasing temperature,

(23) Kimura, T.; Goto, T.; Yamane, H.; Iwata, H.; Kajiwara, T.; Akashi, T. *Acta Crystallogr.* **2003**, *C59*, i128.
(24) Proffen, Th.; Billinge, S. J. L. *J. Appl. Crystallogr.* **1999**, *32*, 572.
(25) Kohara, S.; Suzuya, K.; Takeuchi, K.; Loong, C.-K.; Grimsditch, M.; Weber, J. K. R.; Tangeman, J. A.; Key, T. S. *Science* **2004**, *303*, 1649.

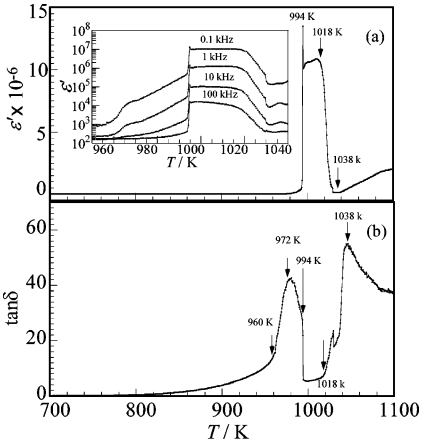

Figure 4. Temperature dependence of (a) permittivity ϵ' and (b) loss component tan δ at a frequency of 100 Hz, showing the temperature dependence of ϵ' at frequencies of 100 Hz, 1 kHz, 10 kHz, and 100 kHz in the inset a.

passing through the glass-transition temperature from 800 K to $T_{\alpha-\text{onset}}$. Subsequently, at $T_{\alpha-\text{onset}}$, the magnitude of ϵ' jumped instantaneously from 10^6 to 1.5×10^7 and then dropped to 1×10^7, within a temperature interval of 1 K and a time interval of 20 s, forming a sharp peak in the permittivity curve. In the temperature range of $T_{\alpha-\text{onset}}$ to $T_{\beta-\text{onset}}$, ϵ' maintained a huge magnitude of 10^7. The magnitude of ϵ' decreased to 10^5 after the α phase translated to the β phase above $T_{\beta-\text{onset}}$. The temperature dependence of ϵ' at 1, 10, and 100 kHz demonstrated the same dielectric anomalies as did ϵ' at 100 Hz around $T_{\alpha-\text{onset}}$ (inset, Figure 4a), but the magnitude of ϵ' was strongly dependent on frequency. The temperature dependence of tan δ exhibited a similar tendency to that of ϵ' when below $T_{g-\text{end}}$. It increased dramatically with temperature, especially in the glass-transition range, and reached a maximum at $T_{g-\text{end}}$. At $T_{\alpha-\text{onset}}$, however, tan δ presented behavior opposite to that of ϵ' and dropped instantaneously by 1 order of magnitude, from 30 to about 3, maintaining this low value over the range from $T_{\alpha-\text{onset}}$ to $T_{\beta-\text{onset}}$. After the phase transition of the α phase to the β phase, tan δ began to increase with increasing temperature.

Ordering Effect. It is interesting to address the question of the mechanisms of the giant dielectric response observed at the crystallization temperature. High-energy X-ray diffraction data revealed the evidence of distorted [TiO_5] polyhedra, so we first fitted the dielectric anomalies' behavior at crystallization with Lines' model.[8] According to Lines' model, the permittivity can be described as

$$\epsilon' = \frac{4\pi\alpha\theta}{1 - 3/4\pi\alpha\theta} \tag{1}$$

where α is the polarizability of the "soft unit", and

$$\theta = 1 + ae^{-\rho(1-t)} - bt \tag{2}$$

where a and ρ are the mode softening parameters, b is an effect of anharmonicity, and $t = T/T_{\text{cryst}}$. If the value of θ at T_{cryst} was $\theta_{\text{cryst}} = 1 + a - b = 4\pi\alpha/3$, the the value of ϵ' would diverge and a ferroelectric transition would occur. With appropriate parameters, we obtained a good fit to the ϵ' data approaching T_{cryst} using eq 1 (Figure 5). Hence, the

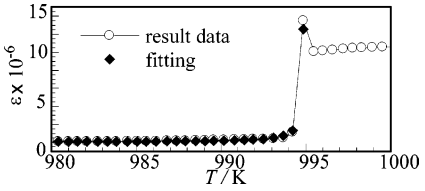

Figure 5. Fit of eq 1 to the data results in approaching $T_{\text{cryst}} = 994$ K with parameters of $a = 0.01$, $\rho = 0.52$, $b = 0.002$, and $\alpha = 0.23683$.

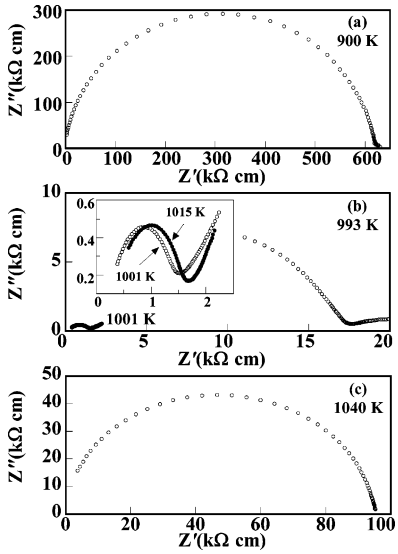

Figure 6. Impedance complex plane plots: (a) 900, (b) 993, 1001, 1015, and (c) 1040 K. The inset in part b presents an expanded view at 1001 K and 1015 K.

giant permittivity of $BaTi_2O_5$ glass appeared to be explained by Lines' model. However, the greater values of tan δ and the significant influence in the frequency of ϵ' reflected the fact that the conductivity of ion movement and the Maxwell−Wagner effect of structural inhomogeneities contributed considerably to the enormous $\epsilon' > 10^7$.

Maxwell−Wagner Effect. To determine the contribution of ion movement and the Maxwell−Wagner effect, the temperature dependence of the impedance of $BaTi_2O_5$ glass was analyzed using impedance complex plane plots (Z^* plots) as shown Figure 6, plotting the imaginary part (Z'') against the real part (Z'). In general, the values of resistance, R, and capacitance, C, of materials can be analyzed by an equivalent circuit of parallel RC elements, which gives rise to a single semicircular arc on the complex plane for a single-phase material. R can be estimated from the diameters of the semicircular arcs, and C can be calculated with the relationship of $\omega_{\text{max}}RC = 1$, where $\omega_{\text{max}} = 2\pi f_{\text{max}}$, and f_{max} is the frequency at the arc maxima.

At room temperature, the R of the glassy $BaTi_2O_5$ was estimated to exceed 10^{12} Ω cm. At 900 K, however, R decreased to 6×10^5 Ω cm, as estimated from the arc in Figure 6a, which suggests that the increase of permittivity and tan δ below $T_{g-\text{end}}$ (Figure 4) was associated with the increase of conductivity of the glass. Above $T_{g-\text{end}}$, two arcs are seen in the response due to the crystallization of the α phase from the glass matrix; one arc corresponds to the α-phase crystal and the other arc corresponds to the glass matrix. Figure 6b depicts the change in the impedance of $BaTi_2O_5$ during α-phase crystallization. At 993 K ($\approx T_{\alpha-\text{onset}}$),

R as identified by the large arc was 1.8×10^4 Ω cm. It dropped by 1 order of magnitude to 1.5×10^3 Ω cm at 1001 K, and maintained this value at 1015 K ($\approx T_{\beta-\text{onset}}$; inset, Figure 6b). This reveals that the jump of ϵ' at $T_{\alpha-\text{onset}}$ corresponded to the drop of R due to the appearance of the α phase. Above $T_{\beta-\text{onset}}$, Z^* plots show a single arc (Figure 6c), meaning that a single β phase appeared; R increased to 10^5 Ω cm at 1040 K. This also suggests that the decrease of ϵ' above $T_{\beta-\text{onset}}$ corresponded to the increase of R due to the disappearance of the α phase. Hence, we believe that the giant dielectric response observed in the temperature range of $T_{\alpha-\text{onset}}$ to $T_{\beta-\text{onset}}$ was due to the existence of the α phase in the glassy matrix. The apparent enormous dielectric constant also could be explained by the Maxwell−Wagner effect of the structural inhomogeneity.

Conclusions

In conclusion, bulk glass of ferroelectric oxide $BaTi_2O_5$ was fabricated without any added network-forming oxide using containerless processing. A new metastable phase that crystallized from the glassy matrix exhibited a $\epsilon' \sim 10^7$. Although glass structure analysis and dielectric data fitting supported the intrinsic ordering model proposed by Lines, an impedance analysis provided obvious evidence of an extrinsic contribution to the apparent permittivity of $\epsilon' > 10^7$ at crystallization. Hence, our results demonstrated that more than one polarization mechanism contributed to the dielectric behavior of $BaTi_2O_5$ glass at high temperature. The interesting phenomenon of the jumping of ϵ' at T_{cryst} at a rate greater than an order of magnitude has important technical implications for obtaining excellent dielectric glass−ceramics through controlled crystallization of $BaTi_2O_5$ glass. We believe that bulk $BaTi_2O_5$ glass will become an important source for fundamental physics study and for practical applications.

Acknowledgment. The authors would like to thank Mr. Y. Saita (Advanced Engineering Service Co., Ltd.) and Mr. H. Masukuni (Chiba Institute of Technology) for fabricating glass samples. Y.K. would like to thank CREST, JST, for the experiment support. The synchrotron radiation experiments were performed at the BL04B2 and BL02B2 in the SPring-8 with the approval of the Japan Synchrotron Radiation Research Institute (JASRI; Proposal No. 2005B0318 and No. 2005B0310).

Supporting Information Available: Rietveld profile fitting of $BaTi_2O_5$ after annealing at 1553 K, crystal parameters of $BaTi_2O_5$ after annealing at 1553 K, and bond length and charge density minimum value of $BaTi_2O_5$ after annealing at 1553 K (PDF). This material is available free of charge via the Internet at http://pubs.acs.org.

CM0525555